18th Brazilian Congress of Thermal Sciences and Engineering
November 16-20, 2020, (online)

ENC-2020-0347

NUMERICAL ANALYSIS OF FLOW BEHAVIOR AND INFLUENCE OF THE REAR SLOPE ANGLE IN AN AHMED'S BODY

Bernardo Silva da Rocha
Charles Rech
Maikson Luiz Passaia Tonatto
Universidade Federal de Santa Maria- campus Cachoeira do Sul, Rodovia Taufik Germano, 3013 - Passo D'Areia, Cachoeira do Sul.
e-mails: besilvarocha8@hotmail.com; charles.rech@ufsm.br; maikson.tonatto@ufsm.br;

Abstract. *Ahmed's body is a simplified geometry of an automobile vehicle used for simulations. In this work, this concept is used to perform a fluid dynamics model of aerodynamic behaviour on the vehicle surface. The aim is to evaluate the flow parameters on an Ahmed's body model and then to test different turbulence models with the same slope angle at vehicle rear. After, the turbulence model is selected which presented the lower variance in the drag coefficient when compared to the other models. The study is made by varying the rear chamfer angle from 10º to 90º, to verify the effect in the drag coefficient. k-£ RNG turbulence model get the value of 0.4066 for drag coefficient and stood out of the other, because it presented the lowest value. Thus, this model is used to study the relationship between the variation of slope angle and the drag of the vehicle, presenting values according to those described in the literature.*

Keywords: *drag coefficient, Ahmed's body, aerodynamics.*

1. INTRODUCTION

One way to evaluate the behavior of aerodynamics profiles is to use the Computacional Fluid Dynamics (CFD). The CFD's function is the study of numerical simulation of phenomena such as fluid flow and heat transfer. It's widely used to obtain pressure, velocity and temperature distributions in the flow region, optimize projects and reduce operating costs, with the objectives achieved in less time and reduce the production of physical prototypes. Besides, this tool can be used to complement theoretical analysis and experimental tests (Fortuna, 2012).

Among the numerical solution methods, the Finite Volume Method (FVM) is widely applied. This method aims to solve the equations of conservation of mass, amount of movement and energy by integrating these equations into control volumes arising from the discretization of the spatial and temporal domain (Maliska, 2004). Besides, in CFD simulations, there are mathematical equations that aim to analyses the presence of flow turbulence. The selection of the appropriate model is important, in order to guarantee an appropriate solution for the flow.

For the validation of turbulence models used in CFD and for studies related to fluid-structure interaction, Ahmed's body is used. Proposed by Ahmed et al. (1984), this is an automobile model with simplified geometry that reproduces the essential characteristics of the flow around a real vehicle, with the exception of the effects arising from the rotation of the wheels, rear-view mirrors and other external elements that make up the bodywork.

Several studies have been carried out using Ahmed's body for the validation of turbulence models through experimental data measured in a wind tunnel (Lienhart and Becker, 2002); for experimental studies on the mat created on the rear surface of the model in non-stationary regime (Sims-Williams and Duncan, 2003); to understand the formation of the mat and the appearance of vortexes, as the angle of departure from Ahmed's body is varied (Gilliéron et al., 2010) and for the validation of the numerical calculation of the drag coefficient of a real vehicle (Rech, 2016).

An important parameter to be evaluated in Ahmed's body is the vehicle's rear slope angle (θ). This parameter has great influence on the aerodynamic behavior of the model, since it's related to the formation of vortex mat structures and, consequently, to the increase of the drag coefficient of the model.

The aim of this work is to carry out and compare the drag coefficient of an Ahmed's body model with a 30º rear slope angle using six different turbulence models and, thus, perform the simulations varying this angle from 10º to 90º, so that it is possible to compare with the experimental results obtained by Hucho and Sovran (1993).

2. MATERIAL AND METHODS

In this work the rear effective slope angle (θ) of Ahmed's body was varied from 10º to 90º in order to obtain the relationship between the variation of this dimension and the appearance of vortices on the rear surface of the vehicle.

The frontal area of all models remained constant at the value of 0.00614 m². Figure 1a illustrates the dimensions of the model and Fig. 1b shows the isometric view of the Ahmed's body with θ equal to 30º.

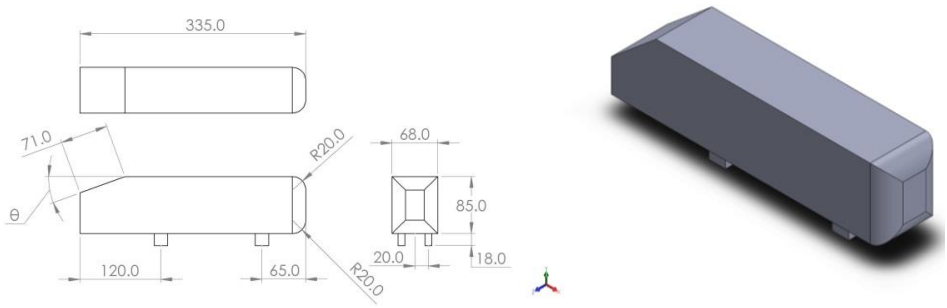

(a) (b)

Figure 1. a) Dimensions [mm] of the model and b) Ahmed's body in 3D, 1:10 scale.

A CFD model was made using ANSYS® FLUENT software. The boundary conditions adopted in the model are shown in Fig. 2a, in which A is the Ahmed's body and B is the face defined as the input speed with a magnitude of 35 m/s. This value was defined by the maximum flow obtained by the fan used in the wind tunnel drive system. Besides, C was defined as the outlet pressure gauge with a value of 0 Pa. In all conditions, the following thermodynamic parameters for air were used: ambient temperature of 15ºC, specific mass of 1.225 kg/m³ and dynamic viscosity of 1.7894×10^{-5} kg/m.s. Regarding the boundary conditions, the non-slip condition was adopted for Ahmed's body, that is, the fluid has a zero velocity in relation to the walls. However, for the *enclosure*, the conditions of stationary wall, shear without slip and standard roughness of the wall were adopted.

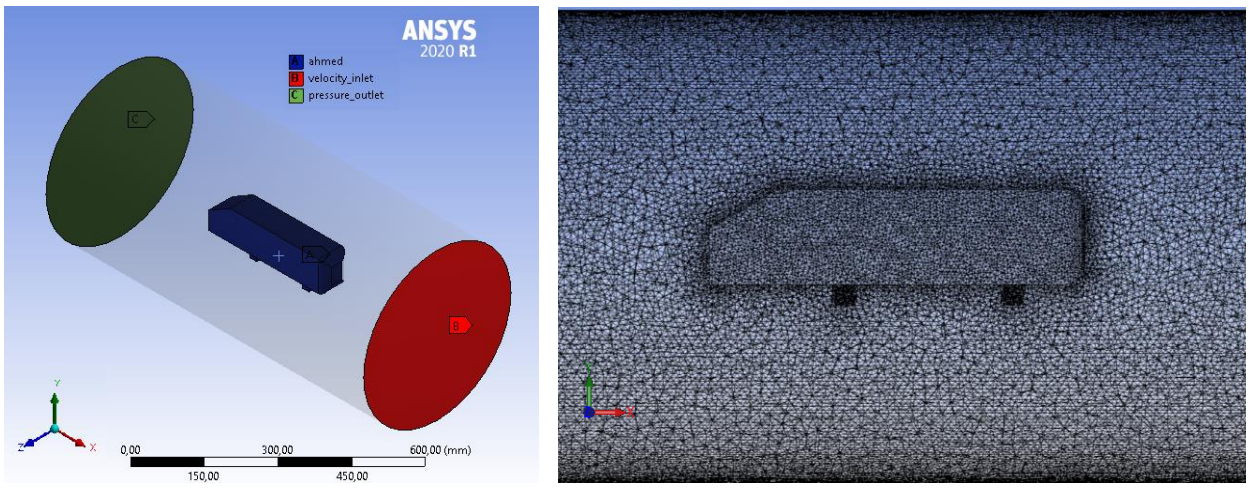

(a) (b)

Figure 2. a) Boundary conditions for the studied models and b) Mesh generated in Ahmed's body, 1:5 scale.

In the mesh convergence study, the tetrahedral mesh method was adopted because it presents the least computational cost. Tests were made with mesh sizes from 100 to 10 mm and the refinement around the model of interest varied from 10 to 3 mm. For this reason, we opted for a tetrahedral mesh in the whole set with 10 mm and around Ahmed's body a refinement of 3 mm was made (Fig. 2b) for a better solution. To reduce computational cost and still obtain the same quality in results, the analysis was performed using the ½ symmetry condition. The mesh generated has a total of 966,509 to 969,850 volumes generated, due to the variation in the slope angle of the rear of Ahmed's body. The Orthogonal Quality mesh verification method recommends that the minimum orthogonal quality be greater than 0.1 and that the average value be in the range of 0.70 to 0.95 (Fluent Incorporation, 2006). For the meshes generated in Ahmed's body, the values found were 0.202 and 0.767, respectively, for the minimum and average orthogonal quality. Therefore, it's evident the generated mesh obtained the expected quality. As the study of the drag coefficient presented in this work occurs in a steady flow, the absolute convergence method was used. This method compares the residual of an equation with the value of the absolute acceptance criterion informed by the user. Standard Fluent values were used: for the energy equation, the absolute acceptance criterion is 10−6 and, for the others, 10^{-3} (Fluent Incorporation, 2006).

The interpolation function used in this work is the UPWIND scheme, proposed by Patankar (1980). Within this method, second-order discretization was chosen because it presents more satisfactory results for tetrahedral meshes

(Versteeg and Malalasekera, 2007). For the pressure-speed coupling, SIMPLE (Semi Implicit Method for Pressure Linked Equations) algorithm was chosen (Patankar, 1980), because it doesn't require the solution of a linear system for the determination of the pressure field (Maliska, 2004). Finally, it was decided to use hybrid initialization, since it's the most used in CFD applications and also guarantees a better forecast of turbulence factors. To initialize the velocity and pressure fields, 10 iterations and an explicit sub-relaxation factor of 1 were used to solve Laplace's equations.

3. RESULTS AND DISCUSSION

3.1 Dimensionless distance from the wall

The parameter that classifies the region of the boundary layer is y+ and this value is important to evaluate whether the mesh refinement close to the walls is adequate. The y^+ values between 0 and 5 are used if the mesh is sufficiently refined to contain elements from the viscous sublayer region, where the boundary layer is calculated in a complete way. Otherwise, it is necessary to construct a mesh in which the centroid is at a dimensionless distance y^+ between 30 and 300, in order to correspond to the region of the logarithmic sublayer of the boundary layer (Kundu and Cohen, 2002). Figure 3a shows the y^+ values found in several turbulence models used in the simulation of Ahmed's body and Figure 3b show the y^+ values for the sphere simulation with different turbulence models.

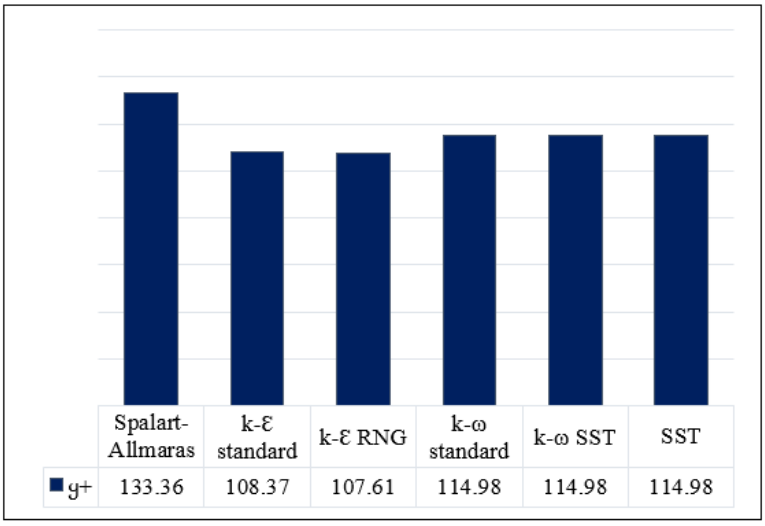

(a)

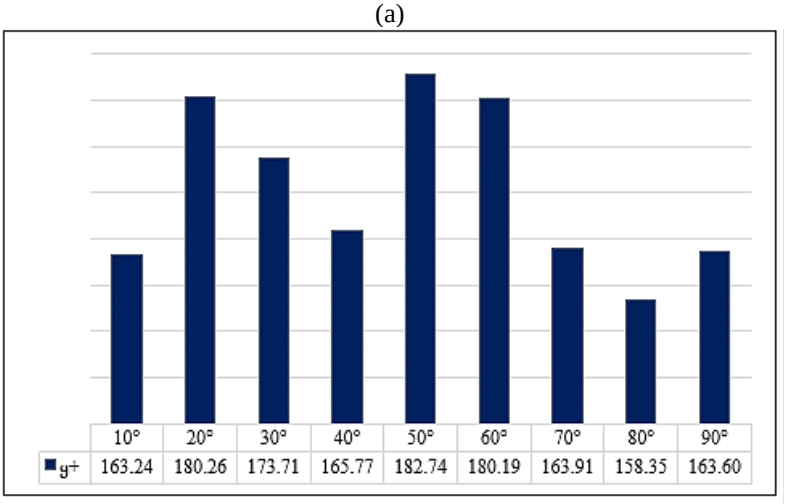

(b)

Figure 3. a) y^+ values for Ahmed's body with 30º and b) y^+ values for Ahmed's body with rear slope angle ranging from 10 to 90º.

It's possible to notice that the Spalart-Allmaras model presented the highest y^+ value. The models of the k – ε family has quite similar values, as do the models of the k − ω and SST group. Both y^+ values provided by different turbulence models for the same rear angle of the vehicle as for different angles and the same turbulence model, are in the range described in the literature as the logarithmic sublayer region (Kundu and Cohen, 2002). Therefore, the refinement adopted in the regions close to the border was satisfactory.

3.2 Numerical analysis for Ahmed's body

For the Ahmed's body with a 30º rear slope angle and using the turbulence models described in the previous sections, the drag coefficient (Cd) values were found using the ANSYS® FLUENT software as shown in Table 1.

Table 1. Ahmed's body drag coefficient with 30° rear slope angle.

Turbulence models	Cd	Cd, pressure	Cd, friction
Spalart-Allmaras	0.4234	0.3732	0.05089
k-Ɛ standard	0.4078	0.3653	0.04246
k-Ɛ RNG	0.4066	0.3666	0.04001
k-ω standard	0.4084	0.3621	0.04635
k-ω SST	0.4150	0.3687	0.04632
SST	0.4130	0.3667	0.04630

Through this analysis, it's noted that there was not a great variation in the drag coefficient between the κ – ε standard, κ– ε RNG e κ – ω standard turbulence models. The κ – ω SST and SST models were also very similar. However, the Spalart-Allmaras model showed greater variation among the others. Table 2 shows the decomposition of the drag coefficient in pressure and friction portions (%).

Table 2. Decomposition of the drag coefficient in pressure and friction portions (%).

	Ahmed et al. (1984)	**Spalart-Allmaras**	**k-Ɛ standard**	**k-Ɛ RNG**	**k-ω standard**	**k-ω SST**	**SST**
Cd, pressure (%)	85	88.0	89.6	90.2	88.7	88.8	88.8
Cd, friction (%)	15	12.0	10.4	9.8	11.3	11.2	11.2

Ahmed et al. (1984) found that about 85% of the total drag was caused by pressure drag and the remaining 15% by friction drag. Therefore, the results provided by the Spalart-Allmaras, κ - ω standard, κ - ω SST and SST models were closer to those found experimentally by Ahmed et al. (1984). Table 3 shows the comparison of the numerical data obtained in the present work with other related published works.

Table 3. Comparison of numerical data obtained in the present work with related works.

Turbulence models	**Authors (2020)**	**Rech (2016)**	**Korkischko (2006)**	**Ahmed et al. (1984)**
Spalart-Allmaras	0.423	0.481	0.404	-
k-Ɛ standard	0.408	0.460	1.618	-
k-Ɛ RNG	0.407	0.451	-	-
k-ω standard	0.408	0.449	-	-
k-ω SST	0.415	0.472	0.384	-
SST	0.413	0.474	-	-
Experimental results	-	-	-	0.378

In comparison with Rech (2016), an analysis was made for the same model. These small variations in the results occurred due to the greater refinement of the mesh used in this work and its quality associated, since Rech (2016) used a tetrahedral mesh with 149,439 volumes generated. In addition, this difference occurs due the use of the fluid speed of 32 m/s and thermodynamic properties referring to the air temperature of 25ºC. In relation to the study proposed by Korkischko (2006), the analysis was performed for an Ahmed's body model 36% smaller than the one proposed in this work, which caused these significant variations between the results, in addition to the associated mesh quality. From an experimental point of view, Ahmed et al. (1984) used a model whose frontal area is larger than that of the model proposed in this work, which resulted in a lower drag coefficient compared to the others.

Because the k-Ɛ standard, k-Ɛ RNG and k-ω standard turbulence models present similar values, it was decided to use one of these models to study the behavior of the drag coefficient of Ahmed's body with the modification of the rear slope angle of the vehicle. The k-Ɛ RNG is the best option because it is one of the most used in the industry and requires less

computational effort, in addition to being widely used in related works (Carregari, 2006; Gonçalves et al., 2018; Rech, 2016). The results obtained are described in Table 4.

Table 4. Drag coefficient for different rear angles from Ahmed's body.

Slope angle (º)	Cd	Cd, pressure	Cd, friction	Cd, pressure (%)	Cd, friction (%)
10	0.199	0.170	0.029	85.2	14.8
20	0.201	0.171	0.029	85.2	14.8
30	0.407	0.366	0.040	90.2	9.8
40	0.291	0.263	0.028	90.1	9.9
50	0.308	0.279	0.028	90.7	9.3
60	0.279	0.251	0.028	89.7	10.3
70	0.214	0.185	0.028	86.6	13.4
80	0.211	0.182	0.029	86.1	13.9
90	0.195	0.165	0.029	84.7	15.3

As the inclination of the rear surface approaches the critical angle (angle of 30º), the two-dimensional flow in the inclined area becomes three-dimensional and the longitudinal vortices become larger. After the critical angle, the flow is separated and the vortex mat becomes practically two-dimensional.

Through this analysis, it's possible to observe that, for a higher aerodynamic drag value, the percentage of pressure drag is higher as well. In addition, models that have lower drag coefficient values have pressure and friction drag portions closer to those found by Ahmed et al. (1984).

Figure 4 illustrates the occurrence of a vortex structure generated on the rear surface of Ahmed's body at a critical angle, which results in a higher drag coefficient of the model with this geometry.

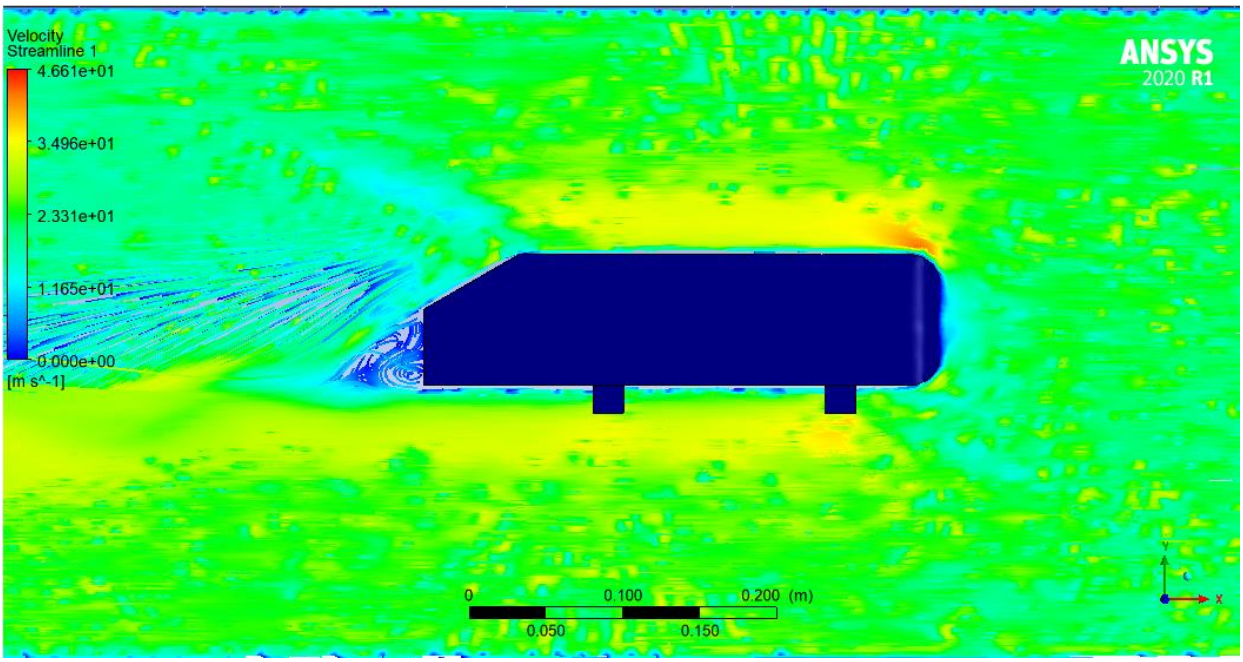

Figure 4. Vortex structure of Ahmed's body with critical rear angle.

Figure 5 shows the comparison of the results obtained numerically with the experimental ones found in Hucho and Sovran (1993).

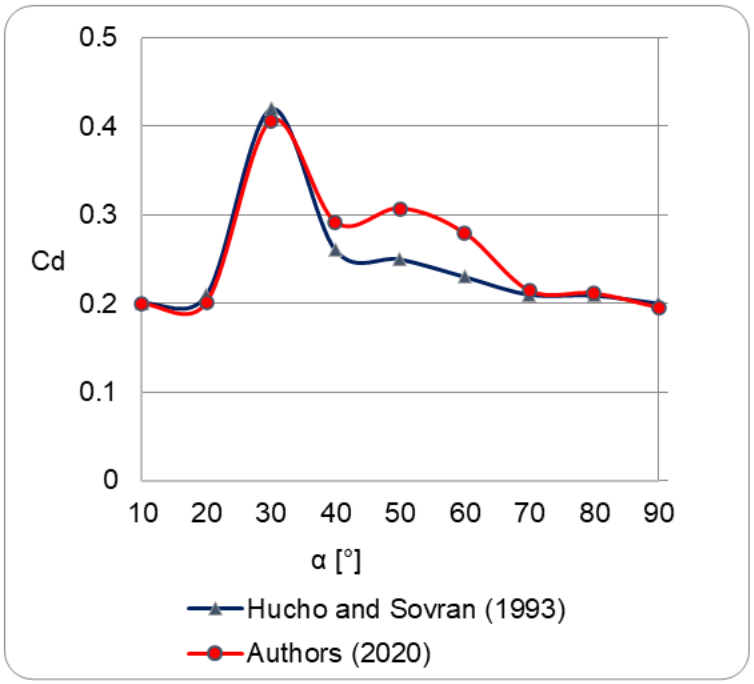

Figure 5. Comparison between numerical and experimental solutions of different Ahmed models.

When comparing the numerical results obtained in this work with the data obtained experimentally by Hucho; Sovran (1993), it can be seen that, in general, the curves are similar. Small variations in the values are known because the model used by the author has a larger frontal area, which results in a lower drag coefficient.

4. CONCLUSION

Ahmed's body shows good agreement for different turbulence models and to reproduce the flow characteristics around conventional vehicles. Besides, the most important parameter to be evaluated in this model is the angle of inclination of its rear surface, since in this region the formation of vortices occurs and, as a result, there is an increase in the drag coefficient of the vehicle.

The numerical analysis of the flow behavior on Ahmed's body surface was performed using six turbulence models. Among these models, k-Ɛ RNG stood out because it's one of the most used in the industry and requires less computational effort. Spalart-Allmaras model, on the other hand, showed the greatest variation among the results. Rech (2016) obtained the same relationship between the turbulence models, although the values found are different due to the use of other parameters, such as fluid speed and air thermodynamic properties.

k-Ɛ RNG turbulence model was chosen for the study of the relationship between drag coefficient and the variation of the rear slope angle of the vehicle because it has the lowest value among the others. Both the numerical simulations performed and the experimental analyses by Hucho and Sovran (1993) obtained a higher drag coefficient with a rear slope angle of 30º. The others results were similar and a few variations occurred because the model studied by the author had a larger frontal area than the model used in this work.

5. REFERENCES

Ahmed, S. R., Ramm, G. and Faltin, G., 1984. *Some salient features of the time-averaged ground vehicle wake*. SAE International, Vol. 93, No. 840300, pp. 473–503.

Anderson, J. D., 2010. *Fundamentals of aerodynamics*. Tata McGraw-Hill Education, New York, 5nd edition.

Carregari, A. L., 2006. *Estudo do escoamento de ar sobre a carroceria de um ônibus usando programa de CFD e comparação com dados experimentais*. Ph.D. thesis, Universidade de São Paulo, São Carlos, Brazil.

Çengel, Y. A. and Cimbala, J.M., 2015. *Mecânica dos fluidos: fundamentos e aplicações*. AMGH Editora Ltda., Porto Alegre, 3nd edition.

Fortuna, A.O., 2012. *Técnicas Computacionais para Dinâmica dos Fluidos: Conceitos Básicos e Aplicações*. Editora da Universidade de São Paulo, São Paulo, 2nd edition.

Fluent Incorporation, 2006. *Fluent 6.3 User's Guide*. Lebanon

Gilliéron, P., Leroy, A., Aubrun, S. and Audier, P., 2010. *Influence of the Slant Angle of 3D Bluff Bodies on Longitudinal Vortex Formation*. Journal of Fluids Engineering, Vol. 132, No. 5, pp. 1–9.

Gonçalves, V. H. P., Oliveira, V. F. and Huebner, R., 2018. *Comparação entre resultados dos modelos de turbulência Spalart-Allmaras, κ–ε e κ–ω SST aplicados na simulação da esteira de vórtices em um modelo simplificado de ônibus rodoviário*. In XIII Simpósio de Mecânica Computacional- XIII SIMMEC 2018. Vitória, Brazil.

Hucho, W. and Sovran, G., 1993. *Aerodynamics of Road Vehicles*. Annual Review of Fluid Mechanics, Vol. 25, No.1, pp. 485–537.

Korkischko, I., 2006. *Investigação experimental e simulação numérica do escoamento ao redor de um modelo automobilístico: corpo de Ahmed*. Undergraduate thesis, Escola Politécnica da Universidade de São Paulo, São Paulo, Brasil..

Kundu, P. K. and Cohen, I. M, 2001. *Fluid Mechanics*. Academic Press, Massachusetts, 2nd edition.

Lienhart, C. and Becker, S., 2002. *Flow and Turbulence Structures in the Wake of a Simplified Car Model (Ahmed Model).* Notes on Numerical Fluid Mechanics, Vol.77, No. 6, pp. 323–330.

Maliska, C.R., 2004. *Transferência de calor e mecânica dos fluidos computacional*. LTC, Rio de Janeiro, 2nd edition.

Patankar, S.V., 1980. *Numerical Heat Transfer and Fluid Flow*. CRC Press, Florida, 1st edition.

Rech, G. M., 2016. *Análise numérica e experimental do comportamento aerodinâmico da carroceria de um ônibus rodoviário*. Master's degree, Universidade de Caxias do Sul, Caxias do Sul, Brasil.

Sims-Williams, D. B. and Duncan, B. D., 2003. *The Ahmed Model Unsteady Wake: Experimental and Computational Analyses.* SAE Technical Paper Series, Vol. 112, No. 6.

Versteeg, H. K and Malalasekera, W., 2007. *An introduction to computacional fluid dynamics: The finite volume method.* Prentice Hall, New Jersey, 2nd edition.

6. RESPONSIBILITY NOTICE

The authors are the only responsible for the printed material included in this paper.